Determination of impedance parameters of individual electrodes and internal resistance of batteries by a new non-destructive technique
2. Theoretical approach

S.A. Ilangovan
Battery Division, Vikram Sarabhai Space Centre, Trivandrum-695 022 (India)

(Received July 13, 1993; accepted November 15, 1993)

Abstract

A novel method to determine non-destructively the impedance parameters of individual electrodes of batteries has been examined. The conditions involve a low rate of constant-current discharge for a short duration and thus no damage is caused to the batteries. The obtained equation is analysed theoretically without any restrictions from approximations. The technique yields the effective double-layer capacitance and charge-transfer resistance of the cathode and the anode separately, as well as the internal resistance of the battery. The correctness of the procedure is verified by simulation studies that permit resolution of the impedance parameters of the anodic and cathodic processes, even if their time constants are not far apart and the parameters are varied widely. Improved battery designs are possible by applying the technique to practical systems.

Introduction

The characterization of battery operation is dependent on impedance parameters such as charge-transfer resistance and double-layer capacitance. These parameters are associated with the individual electrodes, as well as with the internal resistance of the battery. The impedance components are related intimately to the effective area, the kinetics of the electrode processes, and the ion-transport in the battery system. Determination of such fundamental parameters is particularly difficult in the case of sealed batteries, since access to the individual electrodes or the electrolyte is not possible without destroying the battery. Therefore, a more practical approach is to evaluate the impedance parameters by a quantitative and non-destructive technique. Such parameters are most likely to have direct relevance to the design, life, performance characteristics, and eventual failure of battery systems.

Several a.c. methods, as well as d.c. methods, have been used [1–3] to measure the total impedance of the resistive and reactive components of batteries. Besides involving various approximations and assumptions (see below), these methods do not aim at the unambiguous determination of the impedance parameters that correspond to individual electrodes.

Further to work reported previously [4], this study examines theoretically the problem of non-destructive determination of the resistance and capacitance components of cathodes and anodes, as well as the ohmic resistance of batteries with a wide range of capacities and impedance parameters.

SSDI 0378-7753(93)01886-M

Theory

Description of the model

The model for the essential features of battery or cell systems is represented by the electrical equivalent circuit shown in Fig. 1 [4]. In brief, it encompasses a Randles–Ershler model of parallel R–C combination for an electrode/electrolyte interface, component of inductance, Warburg impedance and ohmic resistance.

Background literature

In a.c. impedance studies, the total impedance, Z, is usually the parameter that is measured between the two terminals (shown as heavy dots at the ends of equivalent circuits in Fig. 2) of a battery. Using experimental techniques such as an a.c. bridge [1], the value of Z may be resolved into a series $(R_s - X_s)$ or a parallel $(R_p - X_p)$ combination.

The directly accessible $(R_s - X_s)$ or $(R_p - X_p)$ impedance elements (Fig. 2) are related to individual physicochemical entities that offer impedance (Fig. 1) in a complex way. In order to illustrate this aspect, one may consider, for simplicity, the circuit of Fig. 1 as the case without a diffusion impedance ($Z_{w,1} = Z_{w,2} = 0$) and the assumption that all the impedance elements have a constant value during the experiment. From the standard circuit theory, it can be shown that the net impedance Z of a battery or cell is given in terms of the elements R_s and X_s as:

$$Z = R_s + jX_s \tag{1}$$

where:

$$R_s = R_\Omega + \frac{R_{t,1}}{1+(\omega R_{t,1} C_{d,1})^2} + \frac{R_{t,2}}{1+(\omega R_{t,2} C_{d,2})^2} \tag{2}$$

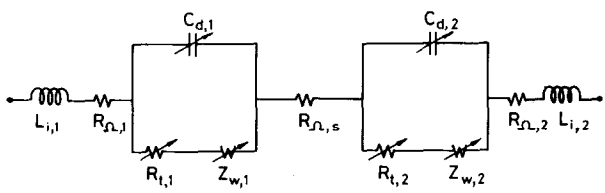

Fig. 1. Generalized equivalent circuit of a battery or cell. $R_{\Omega,1}$, $R_{\Omega,2}$: ohmic resistances of anode (subscript 1) and of cathode (subscript 2), for example, due to grid supports, welds, links etc.; $R_{\Omega,s}$: ohmic resistance of solution and separator; $R_{t,1}$, $R_{t,2}$: charge-transfer resistances of the electrodes; $Z_{w,1}$, $Z_{w,2}$: mass-transfer impedances of electrodes; $C_{d,1}$, $C_{d,2}$: double-layer capacitances of the electrodes; $L_{i,1}$, $L_{i,2}$: self-inductances of the electrodes. Arrows indicate possible dependence on battery or cell voltage and state-of-charge; R_t, Z_w, C_d and L_i above represent only the effective values for porous electrodes since an exact model for the porous structure is unknown. The assignment of subscripts 1 and 2 to anode and cathode is arbitrary.

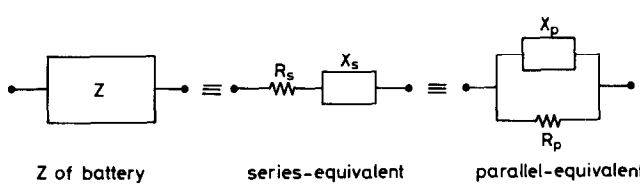

Fig. 2. Equivalent circuit of Fig. 1 resolved into net series and parallel equivalent-circuit elements.

$$X_s = \omega(L_{i,1} + L_{i,2}) - \omega\left(\frac{R_{t,1}^2 C_{d,1}}{1+(\omega R_{t,1} C_{d,1})^2} + \frac{R_{t,2}^2 C_{d,2}}{1+(\omega R_{t,2} C_{d,2})^2}\right) \quad (3)$$

where $\omega = 2\pi f$, and f the frequency in H_2. Similar expressions can be written for the parallel-equivalent elements R_p and X_p.

To extract the desired impedance parameters R_Ω, $R_{t,1}$, $R_{t,2}$, $C_{d,1}$ and $C_{d,2}$, the experimentally accessible values of R_s and X_s at different a.c. frequencies have been made use of in the literature with various degrees of approximations and assumptions [5].

Ideally, a plot of X_s versus R_s (complex plane diagram) should show two well-defined semicircles that correspond to charge-transfer polarization at the two electrodes, as well as a single high-frequency intercept that corresponds to R_Ω on the R_s-axis, in the absence of $L_{i,1}$ and $L_{i,2}$ in eqns. (2) and (3). Such an idealized plot of the complex plane impedance of a battery or cell is not obtained in real systems and the behaviour is quite different to that reported in the literature [3, 6–8].

Assumptions such as those a chosen part of the impedance diagram is a true semicircle, and that this corresponds to only one of the electrodes in the battery or cell, are made usually without any independent proof to calculate the impedance parameters of the individual electrodes. The results are therefore not reliable. In general, a.c. bridge (and related) techniques for the determination of the individual parameters in Fig. 1 suffer from several other limitations, especially the following:

- Clear-cut identification of the contributions from individual electrodes is difficult.
- Multifrequency scanning is mandatory, which is therefore semidestructive to the test battery or cell.
- The self-inductance component of batteries or cells, which is usually seen to be present [9–12] at high frequencies, will affect the value measured as a capacitive reactance and has an unknown error from the inductive reactance at a given frequency.
- Since an a.c. bridge is usually excited by a voltage source of constant amplitude (at different frequencies) the current through the battery or cell under test is not controlled. Such a current could be sufficiently large to cause uncontrolled (and unknown) changes in the state-of-charge on account of: (i) the very small impedance of the system (order of a few milliohms in many practical cases); (ii) the susceptibility of surface films to breakdown (or formation) on the active materials in the electrodes, e.g., films on reactive anodes such as Zn, Mg or Li. Hence, the data obtained do not necessarily refer to the condition of the battery or cell at the beginning of the test. Thus, estimation of impedance parameters ($R_{t,1}$, $R_{t,2}$, $C_{d,1}$ and $C_{d,2}$) of individual electrodes by a.c. impedance data does not seem to be promising.

Frequently, the total internal resistance, R_i, of the battery is the only desired impedance parameter, as this is the direct cause of the dissipative processes in the battery or cell. There are other broad techniques cited in the literature to measure R_i, namely, the current-step [13], the d.c. steady-state [14, 15] and the a.c. impedance techniques. These, despite the limitations, do not aim at determining the impedance parameters that correspond to the individual electrodes. They may be used, however, as an empirical or relative method to assess uniformity in a production line.

Galvanostatic non-destructive test

In order to determine non-destructively the impedance parameters that correspond to the individual electrodes and the interelectrode region (R_Ω, $R_{t,1}$, $R_{t,2}$, $C_{d,1}$ and $C_{d,2}$), test conditions have to be chosen with well-defined and verifiable criteria to:

(i) eliminate diffusion impedances ($Z_{w,1}$, $Z_{w,2}$) and series inductive reactances (due to $L_{i,1}$ and $L_{i,2}$); (ii) ensure that the change in the state-of-charge of the battery or cell is negligible during the test. Also, eliminating diffusion impedances simplifies considerably the theoretical analysis of the problem.

The above requirements may be met readily with the following conditions of the galvanostatic non-destructive test (GNDT). Let the battery, initially at equilibrium, be discharged galvanostatically at an extraordinarily low rate (less than $C_{n/2000}$ A, where C_n is the nominal capacity of the battery in Ah) for a duration not exceeding that at which the voltage falls by about 3 mV (or less) per cell in the battery. The galvanostatic mode eliminates any contribution by the battery or cell series inductance to the measured voltage change. A small perturbation in voltage by about 3 mV, while ensuring a linear polarization domain ($<RT/F$) for the electrodes, will also allow R_t's and C_d's to be considered as constants during the test discharge. A short test duration and the low rate of discharge imply that there will be a time domain within the test duration where the diffusion polarization is negligible compared with charge transfer and ohmic polarization, even at the end of the test*. Finally, the test current and duration ensure that the state-of-charge of the battery or cell changes by less than 0.05% of the initial value, and that any accompanying temperature change is less than a few millidegrees at room temperature.

Consistent with the above GNDT criteria, the equivalent circuit in Fig. 1 can be simplified to that shown in Fig. 3. Under these conditions, the overpotentials** η_1 and η_2 are mainly due to charge-transfer polarization at the two electrodes in their respective linear polarization domain. Let subscripts 1 and 2 denote anode and cathode, respectively. Then, consistent with the convention chosen for the current due to an electrode reaction, namely, cathodic current is positive, it follows that $\eta_1 > 0$ and $\eta_2 < 0$ during discharge of the battery.

Accordingly, from Kirchoff's law:

$$V^r - V - \eta_1 - IR_\Omega + \eta_2 = 0 \tag{4}$$

or,

$$V^r - V = \eta_1 - \eta_2 + IR_\Omega \tag{5}$$

With due regard to the signs of the current (I) at the two electrodes, it follows that at the anode:

$$-I = -C_{d,1}\frac{d\eta_1}{dt} - \frac{\eta_1}{R_{t,1}} \tag{6}$$

and, at the cathode:

$$I = -C_{d,2}\frac{d\eta_2}{dt} - \frac{\eta_2}{R_{t,2}} \tag{7}$$

---

*In the linear polarization domain of an electrode, the magnitude of the diffusion polarization is approximately equal to $[(RT/F)(-I/I_L)]$ when $I_L > I$, where I_L is the instantaneous limiting current at a given instant of time. The instantaneous value of I_L may be approximated to the C_n rate [4, 16]. Therefore, the diffusion polarization is about $26 \times (C_n/2000)/C_n$ mV or 13 μV at the end of the test, at which time the cell voltage changes by about 3 mV according to the test plan. Diffusion polarization will, therefore, be about 13 μV/3 mV, or less than about 0.5%, at the end of the test.

**The overpotential, η, of an electrode is defined as $\eta = E - E^r$ where E is the electrode potential at the given current density, and E^r is the equilibrium potential.

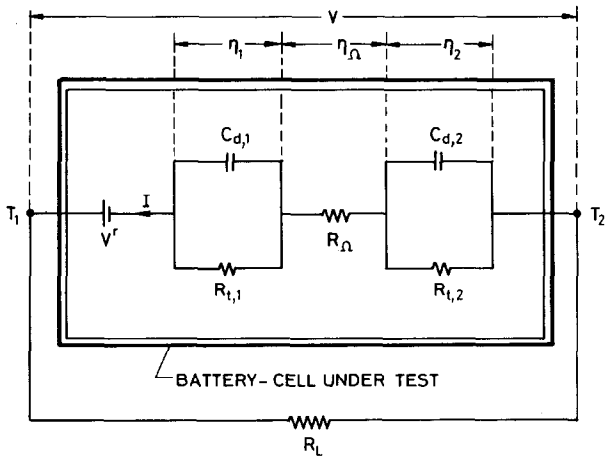

Fig. 3. Equivalent circuit of a battery or cell subjected to discharge under the galvanostatic non-destructive test (GNDT) conditions. V^r: equilibrium e.m.f. of the battery; V: voltage across the terminals T_1, T_2 of the battery-cell when it sustains a constant discharge current I ($I>0$) through a load resistance R_L; η_1: overpotential of electrode 1 at current I; η_2: overpotential of electrode 2 at current I; η_Ω: potential drop across R_Ω ($=IR_\Omega$). Other symbols are as in Fig. 1. The total resistance $R_\Omega = R_{t,1} + R_{t,2} + R_{\Omega,s}$.

On solving eqn. (6) for η_1:

$$\eta_1 = IR_{t,1}[1 - \exp(-t/\tau_1)] \tag{8}$$

where: $\tau_1 = R_{t,1} \times C_{d,1}$.

Similarly:

$$-\eta_2 = IR_{t,2}[1 - \exp(-t/\tau_2)] \tag{9}$$

where: $\tau_2 = R_{t,2} \times C_{d,2}$.

On substituting for η_1 and η_2 in eqn. (5) from eqns. (8) and (9):

$$V^r - V = IR_\Omega + IR_{t,1}[1 - \exp(-t/\tau_1)] + IR_{t,2}[1 - \exp(-t/\tau_2)] \tag{10}$$

If the time constants of the two relaxation processes are widely separated, e.g., $\tau_1 \ll \tau_2$, there is no difficulty in solving eqn. (10). Such a situation cannot, however, be assumed without adequate reasons and is unlikely to be always valid in practical systems.

The general case of comparable time constants with varying combinations of $R_{t,1}$ and $R_{t,2}$ as well as $C_{d,1}$ and $C_{d,2}$ is therefore important. Apparently, even in such a case, the desired resistance and capacitance parameters R_Ω, $R_{t,1}$, $R_{t,2}$, $C_{d,1}$ and $C_{d,2}$ may be obtained by solving eqn. (10) with V–t data. There are, however, serious difficulties in a direct algebraic (or curve-fitting) procedure in solving the problem to obtain a unique and acceptable solution of eqn. (10) for the parameters, when using actual measurements, unless the errors are modelled and suitable correction procedures are incorporated. The solutions obtained are likely to be dubious from a practical point of view [4].

Alternatively, a common approach to solve an exponential equation is to linearize the exponential terms. If this linear approximation procedure with respect to time is

adopted for eqn. (10) by considering only the domain $t \ll (\tau_1; \tau_2)$, it follows that:

$$\frac{V^r - V}{I} = R_\Omega + \left(\frac{R_{t,1}}{\tau_1} + \frac{R_{t,2}}{\tau_2}\right)t \tag{11}$$

This shows that only R_Ω and the composite parameter $(1/C_{d,1} + 1/C_{d,2})$, i.e., the coefficient of t in the above equation, are accessible.

Moreover, the accuracy of the determination of the above quantities is questionable for experimental data since identification of a proper linear domain is generally not possible (due to difficulties in obtaining error-free data in the initial region of measurement). Thus, the main problem of solving for R_Ω, $R_{t,1}$, $R_{t,2}$, $C_{d,1}$ and $C_{d,2}$ remains unsolved.

Present data-processing procedure

A robust data-processing procedure for solving eqn. (10), that is not vulnerable to above approximations, is required when applied to V–t transient data of batteries or cells. Such a procedure is described below.

At the outset of the analysis, it is necessary to identify, from the discharge transient, the region of the diffusion-free zone and linear polarization domain as set out by criteria defined above. This may be easily achieved in the following way. The linear polarization assumption means that $(V^r - V)$ must be proportional to the discharge current I at any time t of discharge, or $[(V - V^r/I]$ versus t should result in a single curve although obtained at different discharge currents up to the time when the polarization exceeds the limit of the linear domain (3 mV) at either the cathode, the anode, or both (Fig. 4). The shaded area in Fig. 4 corresponds to the linear polarization domain.

Next, diffusion polarization is given (see above) by $[(RT/nF)\ \ln(1 - I/I_L)]$. This may be approximated to $[-(RT/nF)I/I_L]$ due to the fact that $I \ll I_L$ for batteries or cells at states-of-charge higher than about 5%. Since I is kept constant and $I_L \alpha t^{-1/2}$ (or $t^{-1/4}$ for all porous electrodes [17, 18]), it follows that if the polarization $(V - V^r)$ is all due to diffusion, then $(V - V^r)$ will be proportional to $t^{1/2}$ (assuming planar diffusion) or to $t^{1/4}$ (assuming diffusion in an all-porous electrode). A situation of

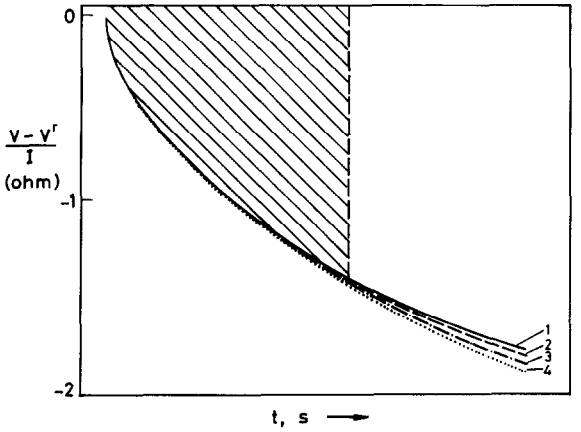

Fig. 4. Schematic curves of $(V - V^r)/I$ vs. t obtained from battery or cell discharge transients at different galvanostatic currents (1 to 4, increasing values).

$(V-V^r)\alpha t^{1/2}$ may therefore be considered as a reasonable description of practical batteries or cells under total diffusion control. Hence, a plot of $(V-V^r)$ versus $t^{1/2}$ can be drawn and that part of graph that lies prior to the onset of a linear dependence of $(V-V^r)$ on $t^{1/2}$ (shown shaded in Fig. 5) may be considered for analysis as this will be without any significant diffusion control.

Further, eqn. (10) shows that V versus t is non-linear. Let two instants of time t^* and t^{**} be chosen in the initial region of the $V-t$ curve (Fig. 6) such that there is a measurable difference in the slopes of the curve (m^*, m^{**}) at these times. The slope in this region is governed by the relaxation processes at both electrodes 1 and 2. Since the coefficients and the indices of the two exponential terms in eqn. (10) have the same sign, the numerical value of the slope of the measured $V-t$ curve is

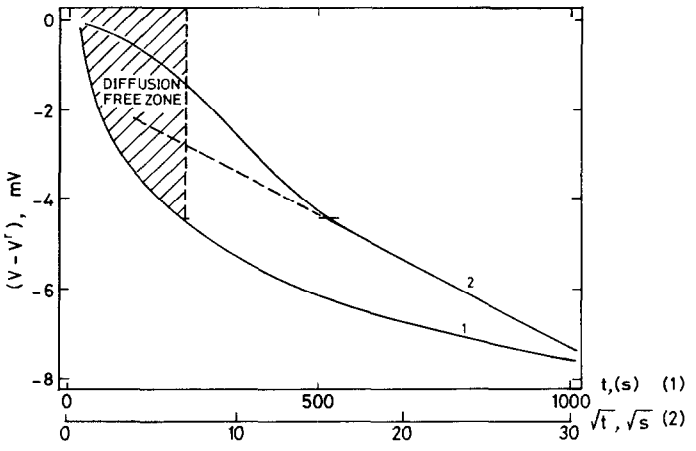

Fig. 5. Schematic graph of $(V-V^r)$ at constant I vs. (1) t and (2) $\sqrt{t}$; the shaded area is free of diffusion control in the porous electrodes.

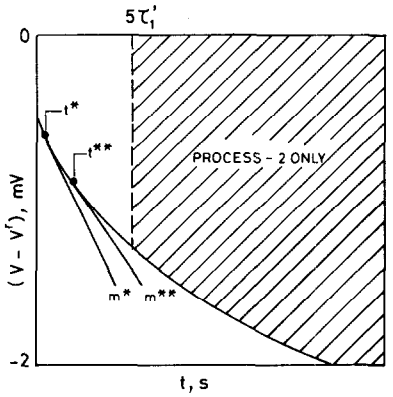

Fig. 6. Typical battery or cell discharge transient under GNDT conditions. t^* and t^{**} are any two arbitrarily chosen points at the beginning of the transient; m^* and m^{**} are the respective slopes of these points. The vertical part of the curve at $t=0(+)$ is generally influenced by inertial effects, switching transients and inductive spikes and, hence, is excluded from the analysis [13]. The test current is of the order of $C_n/3000$ A $-C_n/700$ A where C_n is the nominal capacity, in Ah, of the battery or cell under test.

the numerical sum of the slopes of the two relaxation processes (henceforth designated as: τ_1, process at electrode 1; τ_2, process at electrode 2) in the battery. If it is assumed that the faster of the two is the τ_1 process, then the steady state for the τ_1 process will be approached before that for the τ_2 process.

Step 1

In order to start the analysis, the measured slopes (m^*, m^{**}) in the initial region of the curve may be tentatively assigned entirely to the τ_1 process so that the value of the time constant thus calculated (τ_1') is necessarily equal to, or higher than, the true value (τ_1). The value of τ_1' may be obtained as follows.

On ignoring (temporarily) the exponential term containing τ_2, and differentiating eqn. (10):

$$\frac{d(V^t - V)}{dt} = \frac{IR_{t,1}}{\tau_1'} \exp(-t'\tau_1') \tag{12}$$

Since $(V^t - V)$ is negative for discharge of a battery, then:

$$\ln(-m) = \ln\left(\frac{IR_{t,1}}{\tau_1'}\right) - \frac{t}{\tau_1'} \tag{13}$$

where $m = dV/dt$.

Let $m = m^*$ when $t = t^*$; $m = m^{**}$ when $t = t^{**}$ (Fig. 6), then from eqn. (13):

$$\tau_1' = \frac{t^{**} - t^*}{\ln(-m^*) - \ln(-m^{**})} \tag{14}$$

Since the function $(1 - \exp(-t/\tau))$ attains 99.3% of its final (or steady-state) value at $t = 5\tau$, it follows that the τ_1 process would have practically attained its steady state at $t > 5\tau_1'$.

Step 2

The equation for the transient obtained from eqn. (10) at $t > 5\tau_1'$ is:

$$(V^t - V) = I(R_\Omega + R_{t,1}) + IR_{t,2}[1 - \exp(-t/\tau_2)] \tag{15}$$

Further:

$$\ln\left(-\frac{dV}{dt}\right) = \ln\left(\frac{IR_{t,2}}{\tau_2}\right) - \frac{t}{\tau_2} \tag{16}$$

A linear plot based on eqn. (16) will provide τ_2 and $R_{t,2}$ and, therefore, $C_{d,2}$. Substitution of these parameters in eqn. (15) gives the value of the total resistance R_i $(= R_\Omega + R_{t,1} + R_{t,2})$. The slope will probably yield a more accurate value for $R_{t,2}$.

The parameters $R_{t,2}$, τ_2 and R_i determined above are virtually unaffected by the assignment of the slope in the initial region of the $V-t$ transient to τ_1 process only, since this procedure only overestimates τ_1 and, thereby, identifies accurately the domain governed by the τ_2 process.

Step 3

Equation (10) may now be recast as:

$$Y = -IR_{t,1} \exp(-t/\tau_1) \tag{17}$$

where $Y = V' - V - IR_i + IR_{t,2} \exp(-t/\tau_2)$. Hence:

$$\ln(-Y) = \ln(IR_{t,1}) - t/\tau_1 \quad (18)$$

Estimates of $R_{t,1}$ and τ_1 can be obtained in the domain $t < 5\tau_1'$ according to eqn. (18). A better estimate of $R_{t,1}$ may now be obtained from eqn. (17), which is a straight line through the origin.

Finally, the value of τ_1 thus found may be used as a new or improved value of τ_1', and the calculations from eqn. (15) onward may be repeated until the resulting parameters are constant in two successive calculations. This iterative approach can easily be computerized by putting data in digital form.

All the five parameters (R_Ω, $R_{t,1}$, $R_{t,2}$, $C_{d,1}$ and $C_{d,2}$) of the battery or cell are thus determined individually, accurately and non-destructively by a momentary discharge under galvanostatic conditions at a low rate.

The tacit assumption underlying step 2 is that the contribution by $IR_{t,1} \exp(-t/\tau_1)$ in eqn. (10) is negligible in the time domain $t > 5\tau_1'$. In practical cases, such a conclusion may not always be valid, and even the 0.7% contribution (see step 1) may be significant in comparison with $IR_{t,2} \exp(-t/\tau_2)$, especially when $R_{t,1} \gg R_{t,2}$. In order to allow for such a possibility, the entire analysis can be repeated in the domain $t > n\tau_1$ ($n = 6$, 7, 8, etc.) in step 2 until a constant set of parameters are obtained.

As may be seen from the above analysis, there are four straight line fits, (namely, eqns. (15) to (18)), called for in the data-processing steps. To minimize subjective factors in drawing the straight lines, proper criteria are required, for example, with respect to the range and distribution of data points and the degree of fit. Details of an appropriate data analysis procedure are explained in the Appendix.

Simulation studies

In order to verify the capability of the above analysis procedure to solve the double-exponential form of eqn. (10), simulated voltage–time data were generated by assigning values to all the parameters (essentially to determine the values of these parameters through analysis). For this purpose, a close set (a stringent condition) of relaxation times, viz., 10 s (for τ_1) and 30 s (for τ_2), and different combinations of impedance parameters with wide a range of values were chosen. As the relaxation times were fixed, the ratios $R_{t,1}/R_{t,2}$ and $C_{d,1}/C_{d,2}$ were assigned values in the range 0.01 to 100 and 0.003 to 30, respectively (see Table 1). The magnitudes preferred in the combinations were chosen to reflect the expected value of the impedance parameters of battery systems, in general.

The V–t transient data generated on the basis of the assigned values of impedance parameters were subjected to analysis that followed the procedure detailed above. The required software programme was developed in FORTRAN 77 language. The results are presented in Table 1. A comparison is made between the assigned values of the impedance parameters and those obtained through the method developed in this work. It can be seen that the values of the impedance parameters obtained by analysis of the simulated transients are within 3% of the assigned values over a wide range of the latter. On the other hand, the degree of fit in the linear plots of analysis is somewhat poorer as the ratio of $R_{t,1}$ to $R_{t,2}$ increases beyond about 50, as indicated by the mean absolute deviation values. In most practical cases, $R_{t,1}$ and $R_{t,2}$ may be expected to be within an order of magnitude of each other, and the above difficulty is therefore unlikely to be significant. It is noteworthy that the resolution of impedance parameters may be possible even if $R_{t,1}$ and $R_{t,2}$ vary by about 100 times. Higher

TABLE 1

Comparison of assigned values of impedance parameters with those obtained through the present robust, data-analysis procedure

$\frac{R_{t,1}}{R_{t,2}}$	R_Ω (Ω)	$\tau_1 = 10$ s $= R_{t,1}C_{d,1}$			$\tau_2 = 30$ s $= R_{t,2}C_{d,2}$			Remarks
		$R_{t,1}$ (Ω)	$C_{d,1}$ (F)	ABDEV in τ_1 ($\times 100$)	$R_{t,2}$ (Ω)	$C_{d,2}$ (F)	ABDEV in τ_2 ($\times 100$)	
0.01	0.2	0.2	50		20	1.5		assigned
	0.200	0.200	50.045	0.030	20.000	1.500	0.093	obtained
0.1	0.2	2	5		20	1.5		assigned
	0.199	2.001	4.991	0.053	20.001	1.500	0.106	obtained
1	0.2	0.2	50		0.2	150		assigned
	0.200	0.200	50.002	0.001	0.200	149.999	0.386	obtained
10	0.2	2	5		0.2	150		assigned
	0.199	2.001	4.993	0.039	0.201	149.219	1.517	obtained
50	0.2	10	1		0.2	150		assigned
	0.196	10.003	0.999	0.033	0.204	146.781	6.894	obtained
100	0.2	20	0.5		0.2	150		assigned
	0.198	20.001	0.500	0.008	0.202	148.542	10.927	obtained

$I = 0.01$ A. Time interval between adjacent data points = 0.4 s. Time span = 0 to 300 s. ABDEV = mean absolute deviation found in straight line fits made to obtain the τs.

ratios between $R_{t,1}$ and $R_{t,2}$ could be accommodated with a lower error by improving the precision of the analysis programme.

Other sets of data, similar to Table 1, were constructed in this study for higher values of (τ_2/τ_1), but are not presented here. The results show that the agreement between the assigned and calculated values of the impedance parameters is progressively improved (as expected) as (τ_2/τ_1) is increased beyond 3, i.e., the ratio chosen in Table 1.

The agreement is progressively decreased as the ratio τ_2/τ_1 approaches unity. The case of $\tau_1 = \tau_2$ is, obviously, non-resolvable because then the two exponentials merge with each other, and only the sum $(R_{t,1} + R_{t,2})$, and the products $R_{t,1}C_{d,1} = R_{t,2}C_{d,2} = \tau$ are accessible. This case is easily identified, however, by the linearity of $\ln(dV/dt)$ versus t over the entire time domain.

A measure of the success achieved is demonstrated for a typical experimental GNDT transient in Fig. 7. The excellent agreement between the directly obtained data and the reconstructed curve shows the efficiency of the method to solve the double exponential of eqn. (10) with experimental V versus t data. Further, the phenomenological model proposed for the battery or cell under the GNDT discharge conditions is validated by the above result. It may therefore be concluded that the analysis technique developed in this work to evaluate the individual impedance parameters from V versus t data and eqn. (10) will be highly satisfactory for all batteries or cells except when $\tau_1 = \tau_2$. The latter case is distinguishable easily, even without going through the detailed analysis.

Assignment of subscripts 1 and 2 to anode and cathode, or cathode and anode, may possibly be resolved from the fortuitous experimental results obtained with respect

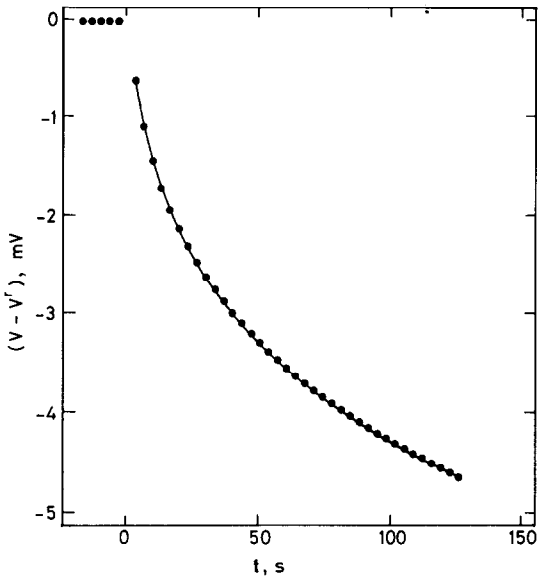

Fig. 7. Typical GNDT discharge transient for sealed lead/acid battery (6 V, 4 Ah) at a constant current of 4.06 mA, with an ageing period of 73 h at 29.8±0.05 °C; SOC=70%. Continuous line is calculated from the parameters of the equivalent circuit evaluated by processing the data points (●) following the procedure described in the text.

to state-of-charge of the battery or cell and by considering the mechanistic concepts of individual electrodes.

Conclusions

1. The above investigations lead to the significant conclusion that the individual values of all the five impedance parameters, namely, charge-transfer resistance of the cathode and of the anode, double-layer capacitance of the cathode and the anode, and the internal resistance of the battery/cell can be determined accurately by the proposed galvanostatic non-destructive test (GNDT). The difficulties involved in determining the above parameters through a.c. impedance method have been analysed.

2. By suitable well-defined and verifiable GNDT criteria, the diffusion impedance and series inductance component of cells that usually distorts the data and complicates the analysis can be rendered negligible.

3. A simple route is provided to solve the double exponential equation (eqn. (10)) from a single transient of voltage–time data. The results obtained are unique, accurate and not restricted by any approximation.

4. Spurious effects due to switching transients, instrument rise time, etc., can be eliminated since the analysis will make use of the data obtained well after the decay of these transients.

5. For the first time, a fundamental framework of parameters for the evaluation, design improvement, cycle life and failure-mode prediction and development strategies for battery systems is provided. This is because the impedance parameters are obtained

as discrete contributions from the cathode, anode and the electrolyte/separator components of batteries.

The GNDT technique has been applied to practical systems, viz., sealed lead/acid, nickel/cadmium, zinc/manganese dioxide and lithium/manganese dioxide batteries, and the impedance parameters of individual electrodes as a function of state-of-charge have been obtained successfully.

Acknowledgements

The author gratefully acknowledges the invaluable guidance and encouragement given by late Professor S. Sathyanarayana and Professor A.K. Shukla.

References

1 W.J. Hamer, in N.C. Cahoon and G.H. Heise (eds.), *The Primary Battery*, Vol. 2, Wiley, New York, 1976.
2 M. Keddam, Z. Stoynov and H. Takenouti, *J. Appl. Electrochem., 7* (1977) 539.
3 Ph. Blanchard, *J. Appl. Electrochem., 22* (1992) 1121.
4 S.A. Ilangovan and S. Sathyanarayana, *J. Appl. Electrochem., 22* (1992) 456.
5 R. Barnard, L.M. Baugh and C.F. Randell, *J. Appl. Electrochem., 17* (1987) 185.
6 M. Keddam, Z. Stoynov and H. Takenouti, *J. Appl. Electrochem., 7* (1977) 539.
7 R. Haak, C. Ogden, D. Tench and S. de Stefano, *J. Power Sources, 12* (1984) 289.
8 S. Sathyaranaya, S. Venugopalan and M.L. Gopikanth, *J. Appl. Electrochem., 8* (1978) 479.
9 B. Savova-Stoynov and Z.B. Stoynov, *J. Appl. Electrochem., 17* (1987) 1150, and refs. therein.
10 S. Sathyanarayana, S. Venugopalan and M.L. Gopikanth, *J. Appl. Electrochem., 9* (1979) 125.
11 M.L. Gopikanth and S. Sathyanarayana, *J. Appl. Electrochem., 9* (1979) 369.
12 M. Hughes, R.T. Barton, S.A.G.R. Karunathilaka and N.A. Hampson, *J. Appl. Electrochem., 15* (1985) 129.
13 M. Hughes, in A.T. Kuhn (ed.), *Techniques in Electrochemistry, Corrosion and Metal Finishing – A Handbook*, Wiley, New York, 1987.
14 J. Millman and C.C. Halkias, *Integrated Electronics: Analog and Digital Circuits and Systems*, McGraw-Hill, Singapore, 1971.
15 D. Goudot, Specifications for nickel-cadmium cells, *Document No. E.W.P. 1155*, European Space Research and Technology Centre, Noordwijk, The Netherlands, Oct. 1978.
16 S. Okazaki, S. Higuchi, N. Kubota and S. Takahashi, *J. Appl. Electrochem., 16* (1986) 513.
17 R. de Levie, *Adv. Electrochem. Electrochem. Eng., 16* (1967) 329.
18 H. Laig-Horstebrock, *J. Electroanal. Chem., 180* (1984) 599.
19 W.H. Press, B.P. Flannery, S.A. Teukolsky and W.T. Vetterling, *Numerical Recipes*, Cambridge University Press, Cambridge, 1986.

Appendix

Straight line fit of data points and 'mean absolute deviation'

Basically, the method involves the use of the median as a more robust estimate of the central value rather than the mean. The mathematical details are available in the literature [19]. The main aspects only are given below.

For a straight line of the form:

$$y(x; a, b) = 1 + bx \tag{A1}$$

where a and b are the intercept and slope of an array of y and x data points (total number N). The merit function to be minimized is $\Sigma_{i=1}^{N}(y_i - a - bx_i)$.

The method followed is to fit the data to a least-square model to get an initial estimate of a and b. Then, the mean absolute deviation (A) is calculated:

$$A = \frac{1}{N}\sum_{i=1}^{N}(y_i - a - bx_i) \tag{A2}$$

The a and b values are adjusted to get a minimum of the quantity A in eqn. (A2). In this way, any large sporadic deviations in the experimental data will be weighed against, and a more reliable straight line fit may be obtained.

In this work, the accepted robust straight line fits constructed as above at various stages of the analysis showed $A < 0.01$, although the upper limit was set at $A < 0.05$ as an acceptance criterion.